JOURNAL OF SOLID STATE CHEMISTRY 104, 215–225 (1993)

^{19}F NMR Investigation of Quenched $Sr_{1-x}Bi_xF_{2+x}$ Solid Solutions: Correlations between Short Range Ordering and Ionic Conductivity

SUH KYUNG SOO, J. SENEGAS, J. M. REAU, M. WAHBI, AND P. HAGENMULLER

Laboratoire de Chimie du Solide du CNRS, Université de Bordeaux I, 351 cours de la Libération, 33405 Talence Cedex, France

Received June 10, 1992; in revised form October 5, 1992; accepted October 7, 1992

A ^{19}F NMR investigation of fluorite-type $Sr_{1-x}Bi_xF_{2+x}$ solid solutions ($0 \leq x \lesssim 0.50$) has been carried out on samples quenched from 700°C. The interpretation of the NMR signal is based on the existence of different fluoride ion sublattices and partial exchange between them at increasing temperature. The NMR study confirms the validity of the clustering process proposed for $Sr_{1-x}Bi_xF_{2+x}$ on the basis of electrical conductivity and neutron diffraction results; i.e., progressive transformation with rising x of 3:2:3:0 into 1:0:3:0 clusters. Furthermore, the ^{19}F NMR investigation has made it possible to show that the interstitial fluorine anions of F′ type ($\frac{1}{2}$, u, $u : u \simeq 0.37$) are responsible for the long range motions in $Sr_{1-x}Bi_xF_{2+x}$.

I. Introduction

The F^- conduction mechanisms in anion-excess fluorite-type solid solutions depend largely on the nature of the clusters which form progressively at rising substitution rates. Their determination based on various and complementary techniques, such as neutron diffraction and ^{19}F NMR, is supported by a clustering model (*1*). In $Ba_{1-x}Bi_xF_{2+x}$, for instance, a clustering process has been proposed from neutron diffraction and conductivity determinations. It consists in a progressive transformation with increasing x of 4:4:3:0 clusters into cuboctahedral 8:12:1:0 units (*2*). A study of the solid solution by ^{19}F NMR has made it possible to confirm the validity of the clustering model (*3*). The four numbers $n_1 : n_2 : n_3 : n_4$ characterizing such a cluster indicate that it is constituted by the association of n_1 vacancies (□) in the normal positions ($\frac{1}{4}$, $\frac{1}{4}$, $\frac{1}{4}$) of the fluorite-type network, with n_2 (F′ ($\frac{1}{2}$, u, $u : 0.36 \lesssim u \lesssim 0.41$), n_3 F″ (v, v, $v : v \approx 0.40$), and n_4 F‴ (v, v, $v : v \simeq 0.30$) interstitial fluorine anions (*1*, *4*).

We later extended our investigations to fluorite-type derived $Sr_{1-x}Bi_xF_{2+x}$ ($0 \leq x \lesssim 0.50$) solid solutions (*5*), where the composition dependence of the electrical properties is very different from that observed for $Ba_{1-x}Bi_xF_{2+x}$. A neutron diffraction study of $Sr_{1-x}Bi_xF_{2+x}$ has made it possible to determine the nature of the interstitial anionic sites and the distribution of the F^- ions present between normal and interstitial sites (*6*). A clustering process has been proposed on the basis of the anionic distribution as a function of x; it illustrates the variation of the electrical properties with composition. It consists in a progressive transformation with rising x of 3:2:3:0 clusters into 1:0:3:0 clusters.

This paper collects the results obtained from a ^{19}F NMR investigation performed on samples obtained under the same experi-

0022-4596/93 $5.00

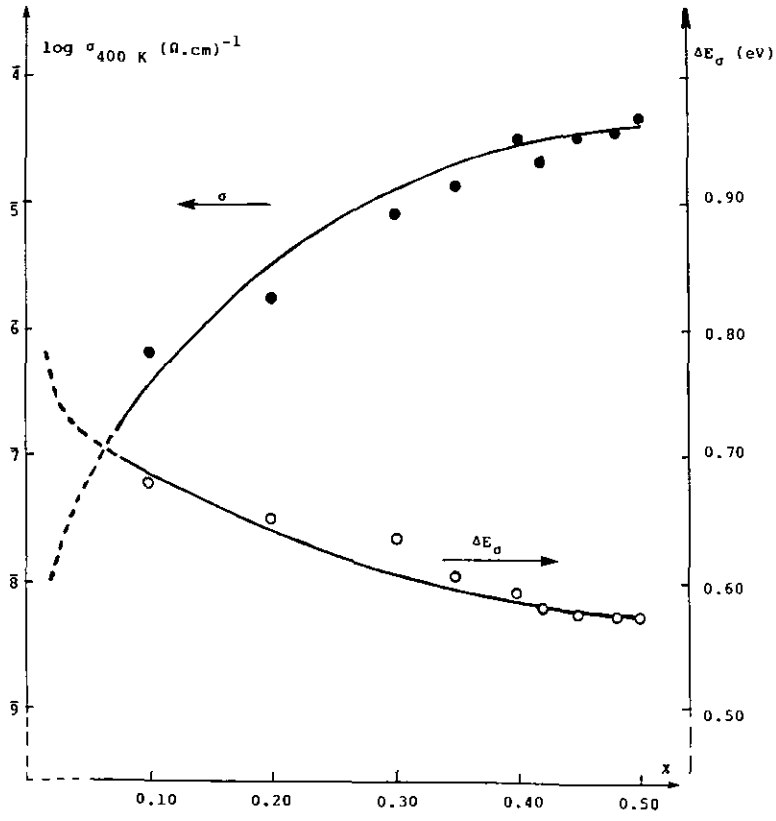

FIG. 1. Composition dependence of log $\sigma_{400\,K}$ and ΔE_σ for the $Sr_{1-x}Bi_xF_{2+x}$ solid solution quenched from 700°C.

mental conditions as for the conductivity measurements and the neutron diffraction study. Valuable information relative to the existence of various possible sites for the F^- ions and to the diffusion of mobile fluoride ions could be expected from such a ^{19}F NMR study and confronted with the ionic conductivity data. Our purpose was to check the validity of the short range model proposed for $Sr_{1-x}Bi_xF_{2+x}$.

II. Reminder of the Electrical Properties of $Sr_{1-x}Bi_xF_{2+x}$ ($0 \leq x \lesssim 0.50$) Solid Solutions Quenched from 700°C

The $Sr_{1-x}Bi_xF_{2+x}$ ($0 \leq x \lesssim 0.50$) solid solutions have been prepared according to (*5*) by synthesis from binary fluorides at 700°C in sealed gold tubes and quenching. $Sr_{1-x}Bi_xF_{2+x}$ is of cubic symmetry; its structure derives from the fluorite-type.

An investigation of electrical properties of $Sr_{1-x}Bi_xF_{2+x}$ solid solutions (*5*) has shown a temperature dependence of the conductivity in agreement with an Arrhenius-type law. The conductivity isotherm at $T = 400$ K and the variation of the activation energy ΔE_σ as a function of x are given in Fig. 1:

—A first domain corresponding to $x \lesssim 0.20$ is characterized by a rather large increase of $\sigma_{400\,K}$ with rising x, associated with a dropping of ΔE_σ.

—For $x \gtrsim 0.20$ the electrical conductivity increases more slowly, tending toward a

maximum. It is difficult to determine clearly this maximum which occurs in any case for a substitution rate x_{max} close to the border substitution rate x_L equal to 0.50.

III. Clustering Process Proposed in $Sr_{1-x}Bi_xF_{2+x}$ ($0 \leq x \lesssim 0.50$)

The large analogy between the composition dependences of the electrical properties of $Sr_{1-x}Bi_xF_{2+x}$ and $Ca_{1-x}Ln_xF_{2+x}$, where Ln^{3+} is a large size rare earth cation (Ln = La, . . . , Gd), has incited us to propose for $Sr_{1-x}Bi_xF_{2+x}$ a clustering process close to that shown in $Ca_{1-x}Ln_xF_{2+x}$ (Ln = La, . . . , Gd) (*7*).

The neutron diffraction investigation of $Sr_{1-x}Bi_xF_{2+x}$ samples quenched from 700°C has revealed the existence of three interstitial anionic sites: F′ ($\frac{1}{2}$, u, $u : u \simeq 0.37$), F″ (v_1, v_1, $v_1 : v_1 \simeq 0.42$), and F‴ (v_2, v_2, $v_2 : v_2 \simeq 0.33$). It has allowed us to determine as a function of x the number of fluoride ions located within the different interstitial sites (Fig. 2) (*6*).

Application of the clustering process model (*1*) has allowed us to determine specific equations for $Sr_{1-x}Bi_xF_{2+x}$ as well as the value of the x_s parameter, the substitution rate for which the number of fluoride ions responsible for long-range motions is maximum, by fitting the experimental data and the calculated values of the number of vacancies and interstitial fluoride ions (Fig. 2). The equations representing $(y_\square)_{tot}$, $(y_{F'})_{tot}$, $(y_{F''})_{tot}$, and $(y_{F'''})_{tot}$, given in Table I,

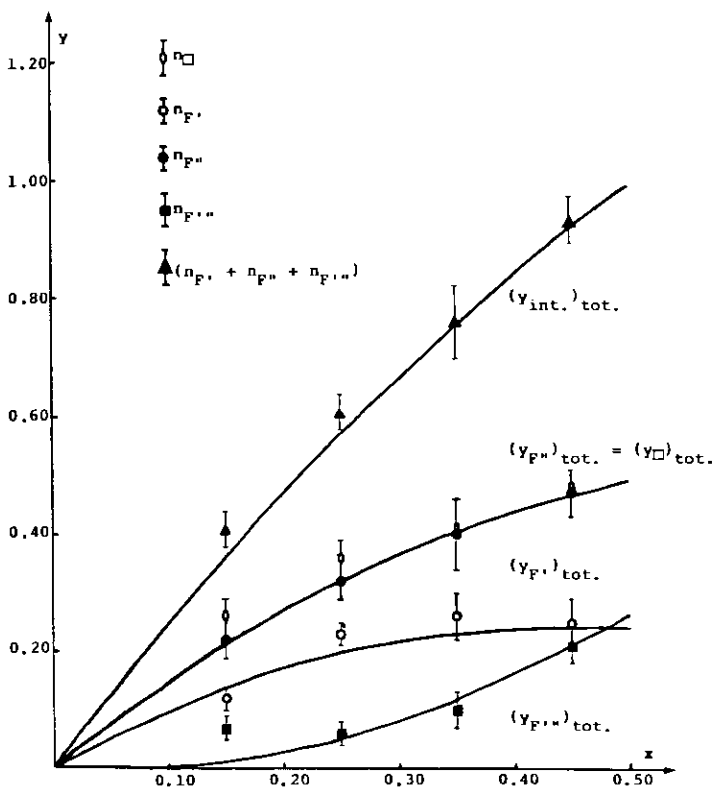

FIG. 2. Experimental values of $n_\square$, $n_{F'}$, $n_{F''}$, $n_{F'''}$, $(n_{F'} + n_{F''} + n_{F'''})$, and graphic representation of the $(y_\square)_{tot}$, $(y_{F'})_{tot}$, $(y_{F''})_{tot}$, $(y_{F'''})_{tot}$ and $(y_{int})_{tot}$ functions relative to $Sr_{1-x}Bi_xF_{2+x}$ (*5*).

TABLE I

ANALYTICAL EXPRESSIONS FOR $(y_{\square})_{tot}$, $(y_{F'})_{tot}$, $(y_{F''})_{tot}$, AND $(y_{F'''})_{tot}$ FOR THE $Sr_{1-x}Bi_xF_{2+x}$ SOLID SOLUTIONS

$$(y_{\square})_{tot.} = \frac{x^3 + 3x_s^2 x}{2(x^2 + x_s^2)}$$

$$(y_{F'})_{tot.} = \frac{2x_s^2 x}{2(x^2 + x_s^2)}$$

$$(y_{F''})_{tot.} = \frac{x^3 + 3x_s^2 x}{2(x^2 + x_s^2)}$$

$$(y_{F'''})_{tot.} = \frac{2x^3}{2(x^2 + x_s^2)}$$

characterize a progressive transformation with rising x of 3:2:3:0 clusters into 1:0:1:2 ones. Steric considerations have nevertheless induced the selection of 1:0:3:0 clusters involving an average (F″)* (v_m, v_m, v_m : v_m = 0.39) position located between the F″ and F‴ sites instead of the 1:0:1:2 clusters (*6*). The value of x_s (x_s = 0.48) is very close to x_{max} (Fig. 1). This result agrees with the clustering model (*1*). As a consequence, $Sr_{1-x}Bi_xF_{2+x}$ is characterized by progressive transformation with increasing x of 3:2:3:0 clusters into 1:0:3:0 ones.

The F′ fluoride ions shown in $Sr_{1-x}Bi_xF_{2+x}$ are represented by the $(y_{F'})_{3230}$ function [$(y_{F'})_{3230} = (y_{F'})_{tot.}$] which attains his maximum for x_s: they can be considered, according to clustering model (*1*), as the interstitial fluoride ions $(F_i)_m$ responsible for long range motions in the solid solutions. The ^{19}F NMR investigation could be expected to confirm such a hypothesis.

IV. ^{19}F NMR Investigation of the $Sr_{1-x}Bi_xF_{2+x}$ ($0 \leq x \leq 0.40$) Solid Solution Quenched from 700°C

The samples correspond to various substitution rates (x = 0.10, 0.20, 0.30, 0.40, 0.45, 0.48, and 0.50). They have been prepared under the same experimental conditions as those used for electrical measurements.

IV. 1. Experimental: High Resolution Solid State NMR

NMR experiments were performed on a BRUKER MSL-200 spectrometer (B_0 = 4.7 T) equipped with a standard variable temperature unit in the temperature range −150 to 150°C.

A "one pulse" sequence program has been used instead of the "Hahn echo" sequence that is generally used for $I = \frac{1}{2}$ nuclei in solids. The reasons for such a substitution are the following:

The fluoride anions in the investigated samples have different diffusion coefficients.

The "one pulse" program, which uses a very short $\pi/2$ pulse length time (0.61 μsec), allowed us to obtain a large domain of the flat central portion in the power irradiation spectrum.

The spectrometer operating conditions were the following:

—Spectrometer frequency: 188.283 MHz.
—Pulse program : 90° pulse width : 0.6 μsec.
: dead time delay (ringdown delay) : 6 μsec.
: recycle delay time : 10 sec.
—Spectral width : 1 MHz.
—Filter width : 2 MHz.
—Size : 8 K.
—Data point : 2 K.

Simulations of the ^{19}F NMR lines were performed using the "LINE-SIM" program provided by BRUKER. This program allows the adjustment of peak position, peak height, linewidth, ratio of Gaussian and Lorentzian functions, and relative proportions of their areas. When a single Gaussian does not fit exactly with the registered spectrum, an appropriate mixing of Gaussian and Lorentzian functions is used for the simulation. It was the case in particular for the spectra concerning the motional narrowing temperature range.

IV. 2. Results

The ^{19}F NMR spectrum at various temperatures is given in Figs. 3a,b,c for some $Sr_{1-x}Bi_xF_{2+x}$ compositions corresponding respectively to $x = 0.10$, 0.40, and 0.50.

Two peaks called p_1 and p_2 are shown at very low temperatures ($T < 200$ K) and can be attributed, whatever the value of x, to fluoride ions localized respectively in normal sites of the fluorite-type lattice and outside those positions; their contribution is temperature independent, which means that all F^- ions present are fixed in the NMR time scale in this temperature domain.

Above a T_1 temperature a new peak called p_m located between the p_1 and p_2 peaks can be observed. It grows with rising temperature; it represents the fluoride ions which are mobile above T_1.

The relative contributions of the three peaks observed at each temperature are de-

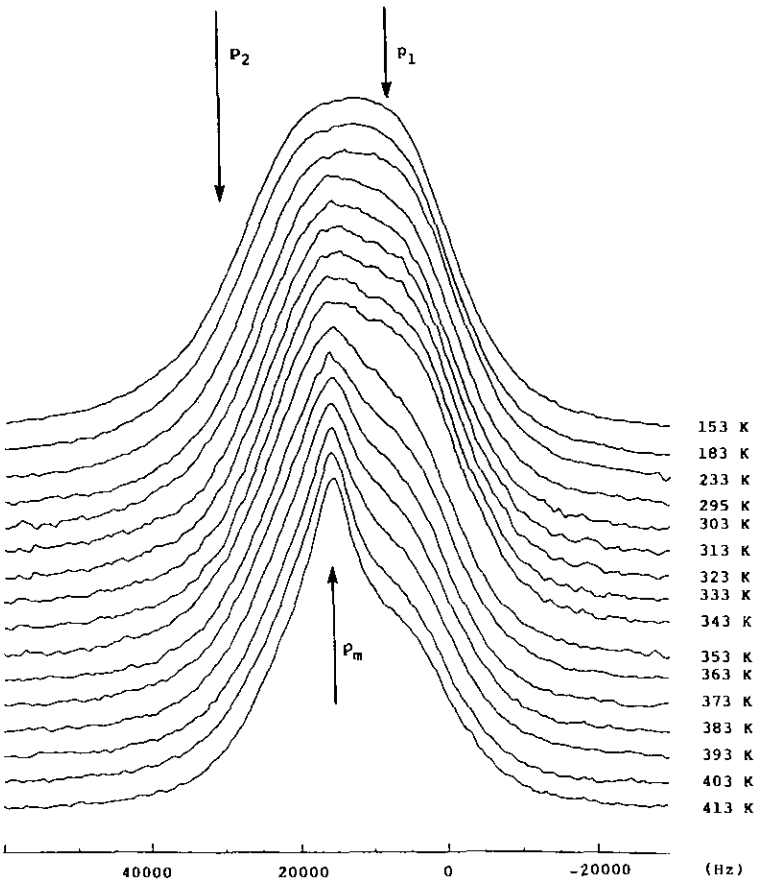

FIG. 3a. Thermal variation of the ^{19}F NMR spectrum for the $Sr_{0.90}Bi_{0.10}F_{2.10}$ composition.

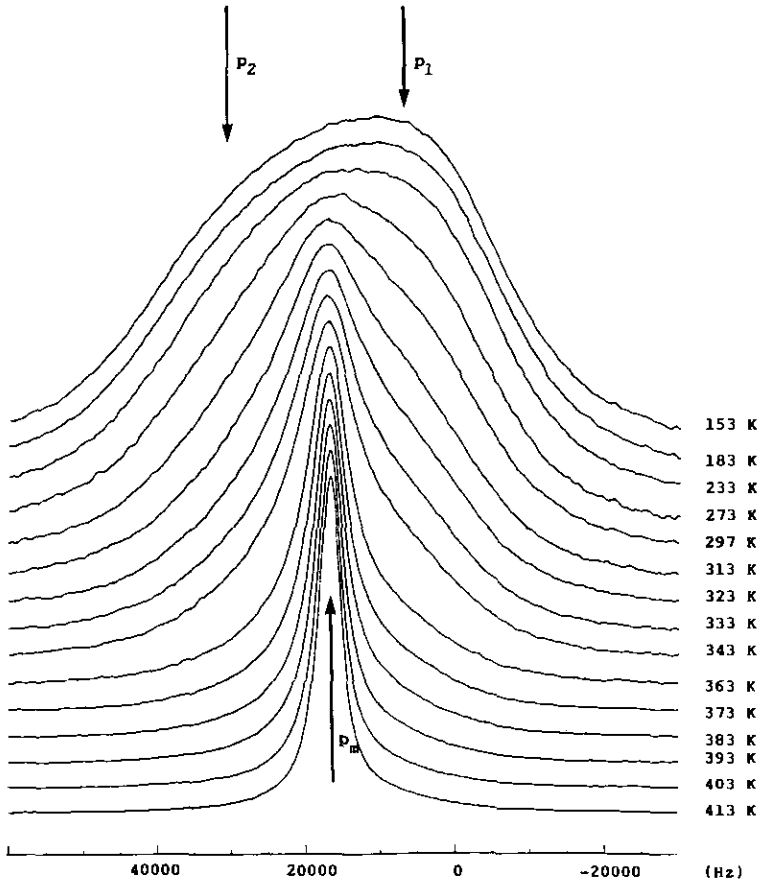

FIG. 3b. Thermal variation of the ^{19}F NMR spectrum for the $Sr_{0.60}Bi_{0.40}F_{2.40}$ composition.

termined by deconvolution of the whole spectrum. Figure 4 gives, as an example, the deconvolution of the ^{19}F NMR spectrum at 273 K and 333 K for the $Sr_{0.60}Bi_{0.40}F_{2.40}$ composition. The temperature dependence of the fluoride ion rates considered as proportional to the areas of the p_1, p_2, and p_m peaks is given respectively in Figs. 5a,b,c for $x = 0.10$, 0.40, and 0.50.

Above T_1, the temperature where p_m appears, the p_2 and p_m peaks merge progressively at rising temperature (Fig. 3); this phenomenon results from an increase of the number of mobile fluoride ions and from a simultaneous decrease of the amount of nonmobile fluoride ions of p_2 type (Fig. 5).

Above a new temperature T_2 ($T_2 > T_1$), p_1 coalesces in turn with p_m when the temperature increases (Fig. 3). This means that the number of mobile fluoride ions now increases quickly not only at the expense of the fluoride ions of p_2 type, but even more at the detriment of F^- ions of p_1 type.

The T_1 and T_2 temperatures, given in Table II, cannot be determined with a high accuracy. Nevertheless, it appears clearly that T_1 and T_2 are the lowest values for $x = 0.40$.

In the investigated high temperature domain, no horizontal plateau has been detected, whatever the value of x, in the temperature dependence of the amount of p_2

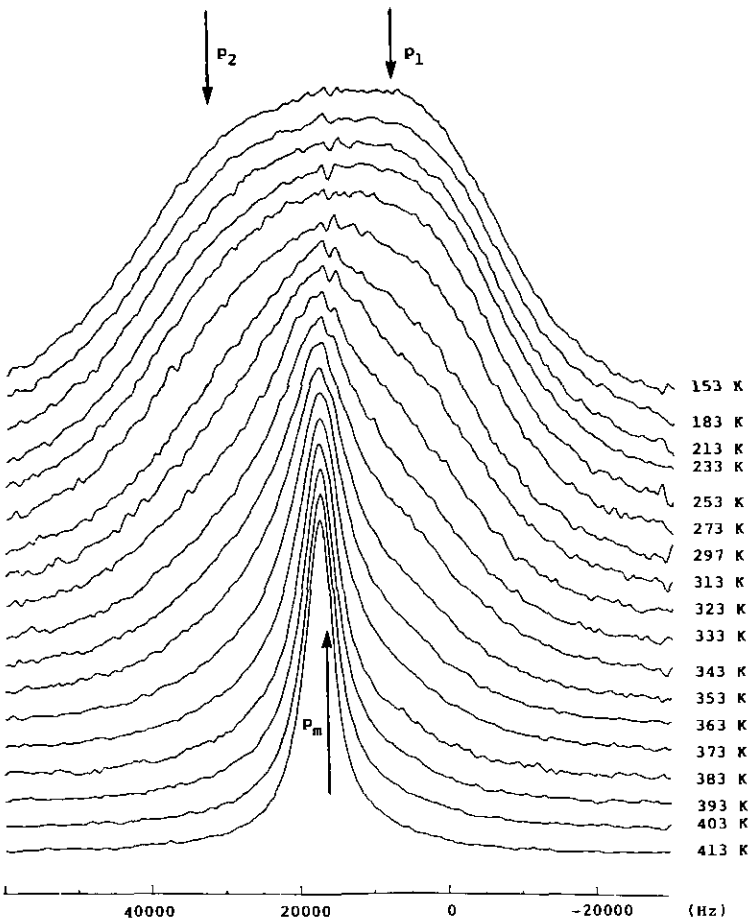

FIG. 3c. Thermal variation of the ^{19}F NMR spectrum for the $Sr_{0.50}Bi_{0.50}F_{2.50}$ composition.

type fluoride ions. Consequently, all interstitial fluoride ions appear, at the NMR scale, to be mobile at increasing temperature in $Sr_{1-x}Bi_xF_{2+x}$. This result distinguishes clearly $Sr_{1-x}Bi_xF_{2+x}$ from $Ba_{1-x}Bi_xF_{2+x}$, for which a horizontal plateau has been observed at high temperature, indicating that the interstitial anions belonging to the cubooctahedral 8 : 12 : 1 : 0 clusters are even fixed at 400 K (*3*).

TABLE II

VALUES OF THE T_1 AND T_2 TEMPERATURES FOR VARIOUS COMPOSITIONS OF THE $Sr_{1-x}Bi_xF_{2+x}$ SOLID SOLUTIONS

x	T_1	T_2
0.10	≈261 K	≈333 K
0.30	≈245 K	≈303 K
0.40	≈238 K	≈284 K
0.45	≈244 K	≈290 K
0.50	≈247 K	≈295 K

In a relatively large temperature domain the p_m line can be considered in Figs. 5a and c as the sum of two lines corresponding to the coexistence of two exchange mechanisms between fluoride sublattices, the nature of which is close but differs slightly. In contrast, in Fig. 5b only one line appears for $x = 0.40$: both effects seem to be aver-

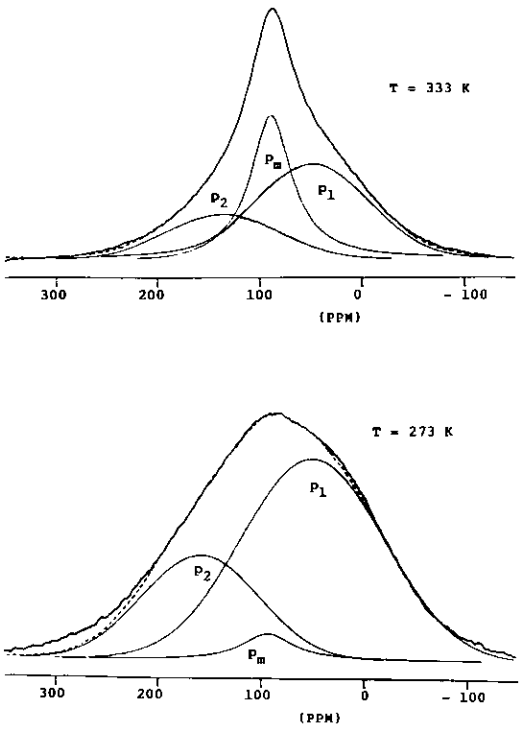

FIG. 4. Deconvolution of the ^{19}F NMR spectrum at 273 and 333 K for $Sr_{0.60}Bi_{0.40}F_{2.40}$ (—: deconvoluted spectrum).

aged for this substitution rate. They correspond to the lowest values of T_1 and T_2 and the largest numbers of mobile ions at the highest temperature considered.

V. Correlations Using the Clustering Model between Results Derived from ^{19}F NMR and Neutron Diffraction

By extrapolation of p_2 at low temperature, the percentage of fixed interstitial fluoride ions can be deduced for each composition. Table III makes it possible to compare these percentages to those deduced from the model and those determined by neutron diffraction. A good agreement is observed.

The mobile fluoride ion percentage at the temperature T_2 can be evaluated from Fig. 5. It has been compared in Table IV to the

TABLE III

COMPARISON OF THE INTERSTITIAL FLUORIDE ION PERCENTAGES DETERMINED BY ^{19}F NMR AT LOW TEMPERATURE WITH THOSE CALCULATED FROM THE MODEL AND THOSE DETERMINED BY NEUTRON DIFFRACTION

	NMR p_2 ($T < T_1$)	Model $(y_{int})_{tot}$%	Neutron diffraction $\frac{100\,(n_{F'} + n_{F''})}{2+x}$
0.10	12%	11.7%	
0.15		16.8%	19.1%
0.25		25.4%	27.1%
0.30	28%	28.9%	
0.35		32.1%	32.3%
0.40	33%	34.8%	
0.45	35%	37.3%	37.9%
0.50	37%	39.6%	

percentage of interstitial fluoride ions of F′ type $[(y_{F'})_{tot.}\%]$ calculated from the model. A fair agreement is observed between the calculated and experimental values (Fig. 6 and Table IV). As a consequence the fluoride ions responsible for long range motions in $Sr_{1-x}Bi_xF_{2+x}$ appear to be the interstitial anions of F′ type.

The ^{19}F NMR investigation has shown, on the other hand, that the carrier mobility is the largest for $Sr_{0.60}Bi_{0.40}F_{2.40}$: the graph of the p_m signals at 413 K observed for the different substitution rates, reported with

TABLE IV

PERCENTAGES OF INTERSTITIAL FLUORIDE IONS MOBILE AT THE T_2 TEMPERATURE DETERMINED BY ^{19}F NMR AND PERCENTAGES OF INTERSTITIAL FLUORIDE IONS OF F′ TYPE CALCULATED FROM THE MODEL

x	NMR p_m at T_2	Model $(y_{F'})_{tot}$%
0.10	5%	4.6%
0.30	8%	9.4%
0.40	8%	9.8%
0.45	8%	9.8%
0.50	8%	9.6%

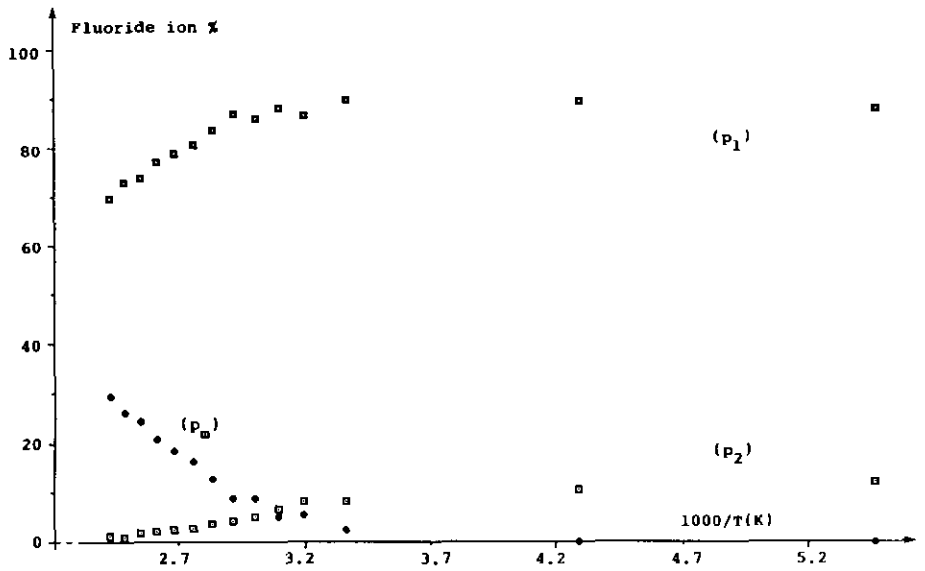

FIG. 5a. Temperature dependence of the fluoride ion rates assumed to be proportional to the p_1, p_2, and p_m peak areas for $Sr_{0.90}Bi_{0.10}F_{2.10}$ ($\Delta p = \pm 2$).

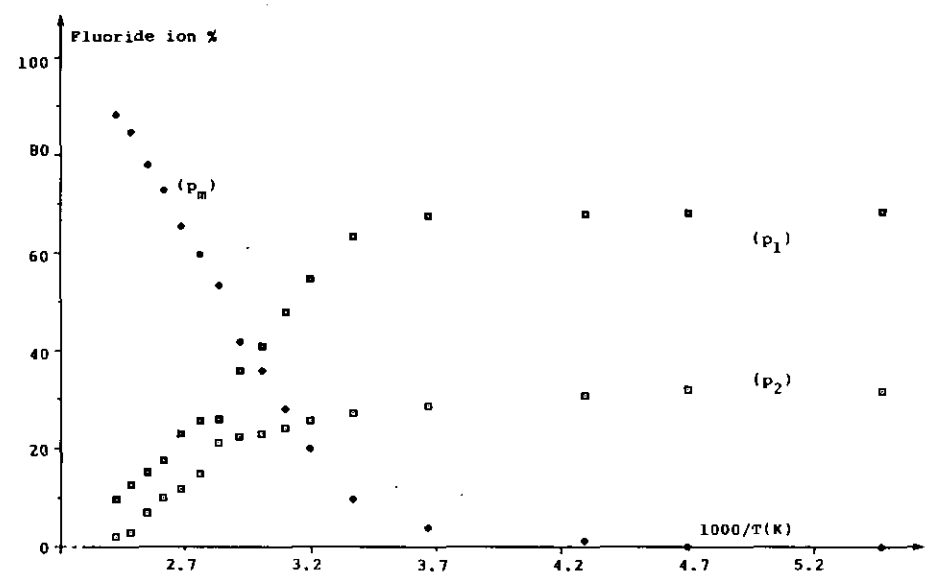

FIG. 5b. Temperature dependence of the fluoride ion rates assumed to be proportional to the p_1, p_2, and p_m peak areas for $Sr_{0.60}Bi_{0.40}F_{2.40}$ ($\Delta p = \pm 2$).

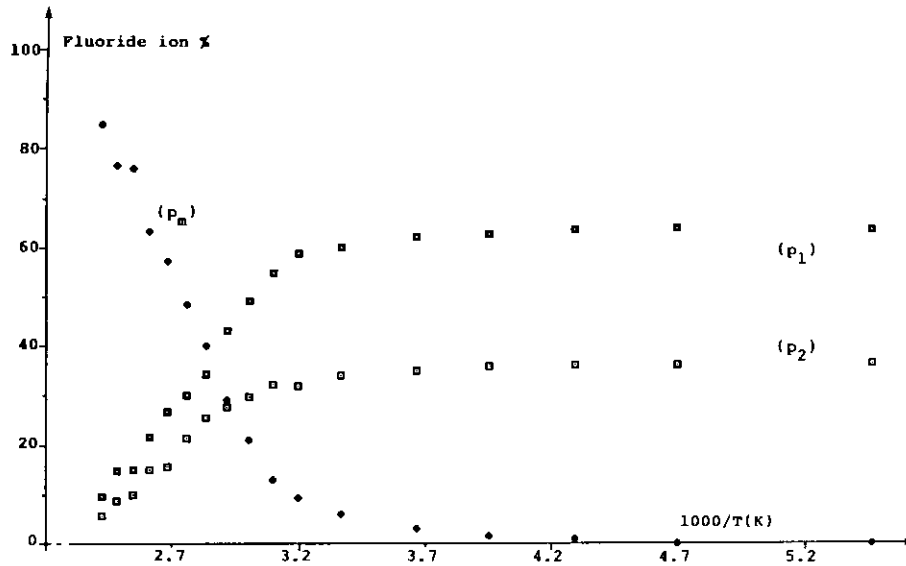

FIG. 5c. Temperature dependence of the fluoride ion rates assumed to be proportional to the p_1, p_2, and p_m peak areas for $Sr_{0.50}Bi_{0.50}F_{2.50}$ ($\Delta p = \pm 2$).

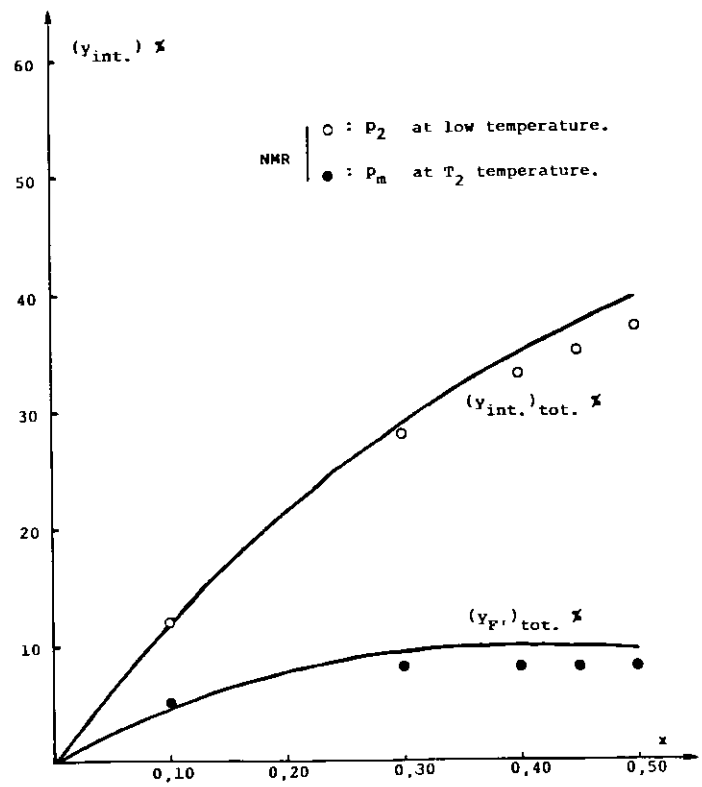

FIG. 6. Experimental percentages of interstitial fluoride ions fixed at low temperature (p_2) and mobile at the T_2 temperature (p_m) determined by ^{19}F NMR ($\Delta p = \pm 2$) and graphic representation of the $(y_{F^-})_{tot}$% and $(y_{int})_{tot}$% functions for $Sr_{1-x}Bi_xF_{2+x}$.

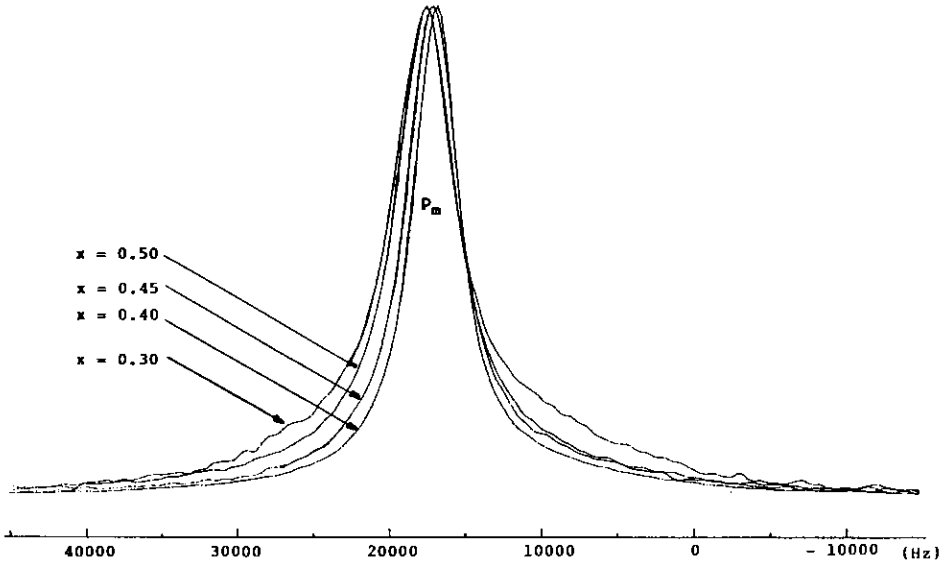

FIG. 7. Comparison of the p_m lines at 413 K relative to various $Sr_{1-x}Bi_xF_{2+x}$ compositions.

the same scale in Fig. 7, indicates clearly that the smallest linewidth is actually obtained for $x = 0.40$.

VI. Conclusions

The ^{19}F NMR investigation of the $Sr_{1-x}Bi_xF_{2+x}$ ($0 \leq x \leq 0.50$) solid solutions has revealed the existence of several fluoride sublattices that become mobile at increasing temperature.

Correlations have been established using a clustering model between the results obtained by NMR and neutron diffraction determinations. The clustering process proposed for $Sr_{1-x}Bi_xF_{2+x}$ on the basis of the anionic distribution as a function of x and of the composition dependence of the ionic conductivity has been confirmed.

The NMR study has allowed us to identify the nature of the first fluoride sublattice mobile at increasing temperature: the fluoride ions responsible for long range motions in $Sr_{1-x}Bi_xF_{2+x}$ are in the model the interstitial anions of F′ type.

References

1. J. M. RÉAU, M. WAHBI, J. SÉNÉGAS, AND P. HAGENMULLER, *Phys. Status Solidi B* **169,** 331 (1992).
2. J. L. SOUBEYROUX, J. M. RÉAU, M. WAHBI, J. SÉNÉGAS, AND SUH KYUNG SOO, *Solid State Commun.* **82,** 63 (1992).
3. SUH KYUNG SOO, J. SÉNÉGAS, J. M. RÉAU, M. WAHBI, AND P. HAGENMULLER, *J. Solid State Chem.* **97,** 212 (1992).
4. A. K. CHEETHAM, B. E. F. FENDER, B. STEELE, R. I. TAYLOR, AND B. T. M. WILLIS, *Solid State Commun.* **8,** 171 (1970).
5. J. M. RÉAU, A. RHANDOUR, S. MATAR, AND P. HAGENMULLER, *J. Solid State Chem.* **55,** 7 (1984).
6. J. L. SOUBEYROUX, J. M. RÉAU, M. WAHBI, J. SÉNÉGAS, AND SUH KYUNG SOO, *Solid State Commun.* **83,** 259 (1992).
7. J. M. RÉAU, J. SÉNÉGAS, AND P. HAGENMULLER, *in* "Proc. ICAM 91, EMRS 1991, Conf. A2–V8, Strasbourg, 1991."